CoFeB Spin Polarizer Layer Composition Effect on Magnetization and Magneto-transport Properties of Co/Pd-based Multilayers in Pseudo-Spin Valve Structures

T. Tahmasebi[1,2], S.N. Piramanayagam[1,a)], R. Sbiaa[1], T. C. Chong[2,3]

[1]Data Storage Institute, A*STAR (Agency for Science, Technology and Research), 5, Engineering Drive 1, Singapore 117608.

[2]Department of Electrical and Computer Engineering, National University of Singapore, Singapore 117576.

[3]Singapore University of Technology and Design, 20 Dover Drive, Singapore 138682, Singapore.

[a)]Author to whom correspondence should be addressed; electronic mail: Prem_SN@dsi.a-star.edu.sg

Abstract

In this work, we used $Co_xFe_{80-x}B_{20}$ (x= 60, 40, 20) as spin-polarizing layers (SPL) in order to investigate the composition of the CoFeB-SPL on the magnetoresistance (MR) in Co/Pd multilayers-based pseudo-spin-valves (PSV) with perpendicular magnetic anisotropy (PMA). In both soft layer (SL) and hard layer (HL), the PMA was achieved by tuning the interface anisotropy and bulk anisotropy between SPL and Co/Pd multilayers. For all the films, giant magnetoresistance (GMR) was found to decrease with SPL thickness in the as-deposited case, irrespective of the CoFeB atomic composition and M_s. However, interesting behavior is observed when the films were annealed. Although GMR degradation is expected after annealing, a peak of GMR was observed after post annealing the samples at 250 ºC. This peak is stronger for the samples with thicker SPLs than those with thinner SPLs. Nonetheless, further increase in annealing temperature causes a reduction in GMR which is found to be larger in Co rich atomic composition samples with a lower M_s. In the case of thicker CoFeB SPL (15 Å), the magnetization of overall composite (Co/Pd)/CoFeB soft layer appears to be canted from out of plane direction. Among the three compositions investigated, $Co_{60}Fe_{20}B_{20}$ polarizer shows a stronger PMA due to its lower M_s, leading to the weaker demagnetization. In addition, this study also indicates that the crystallographic texture of Co/Pd multilayers plays a role in the MR.

I. Introduction

Giant magnetoresistive (GMR) devices based on layers with in-plane anisotropy suffer from switching field fluctuations and cell instability at the edges of nanostructures. Therefore, GMR structures based on layers with perpendicular magnetic anisotropy (PMA) have attracted intense research recently, as they provide better thermal stability and uniform magnetization switching for potential applications in MRAM or other spintronic devices.[1, 2]

Alloys of $L1_0$ FePt or CoPt, Co-based/Pd or Co-based/Pt multilayers are among the most important magnetic materials with PMA for high density memory or storage applications. $L1_0$-based magnetic materials are difficult to be fabricated, as high deposition temperature is needed in order to transform face-centered-cubic (fcc) phase to face-centered-tetragonal (fct) phase for achieving the PMA.[3, 4] However, multilayers with PMA have been intensively investigated as they can be prepared at room temperature. Moreover, the switching field separation between the magnetic layers could be tailored easily by varying the thickness ratio and deposition pressure of the Co and Pd layers.[5, 6] Besides the thickness ratio between Co and Pt and deposition conditions, it is known that the properties of magnetoresistive devices such as GMR, switching field (coercivity) and anisotropy of the ferromagnetic layers are strongly influenced by their film thickness,[7, 8] surface roughness,[9] crystallinity[10] and the type of seed layer.[8, 11]

As reported in literature, magnetic properties and GMR signal in the PSV systems are strongly affected by the property of the spin polarizer layer (SPL).[12, 13] Different SPLs, e.g. Co, Fe, CoFe, adjacent to the spacer layer has been used in order to improve the GMR signal, PMA and switching fields in PSV systems with PMA. Soft magnetic material, e.g. CoFeB films with a high spin polarization,[14] also could be used in PSV devices based PMA, since CoFeB helps in achieving good crystallinity of MgO in magnetic tunnel junction (MTJ), in addition to excellent magnetic properties and large tunneling magnetoresistance (TMR) signal. Although there are numerous research works on MgO tunnel barrier and CoFeB magnetic layer for in-plane anisotropy devices, no systematic study has been carried out on the effect of CoFeB-SPL properties in PSV systems until now. Therefore, in this paper, we investigate the GMR dependence on different thicknesses and saturation magnetization of $Co_xFe_{80-x}B_{20}$-SPL on the magnetic and electric properties of the single spin valve structures.

EXPERIMENTAL DETAILS

Perpendicular PSV with the structure of Substrate/Ta(50Å) /Pd(50Å) /[Co (6Å) /Pd(8Å)]$_2$ / $Co_xFe_{80-x}B_{20}$ (t Å) /Cu(20Å) / $Co_xFe_{80-x}B_{20}$ (t Å)/ [Pd(8Å) /Co(3Å)]$_{10}$ /Pd(30Å) /Ta(50Å) were deposited on thermally oxidized Si wafers using direct current (DC) magnetron sputtering. [Co (6Å) /Pd(8Å)]$_2$ is the soft layer and [Pd(8Å) /Co(3Å)]$_{10}$ is the hard layer. The ten numbers of repeats in bilayers of Pd/Co at the hard magnetic layer were used in order to provide sufficient signal for X-ray diffraction (XRD) measurements and to provide a sufficiently higher anisotropy than the soft layer with fewer repeats. $Co_xFe_{80-x}B_{20}$ was used as spin polarizer layer (SPL) where the Co rich or Fe rich compositions were provided by varying the x from 20%, 40% and 60%. The thickness of $Co_xFe_{80-x}B_{20}$ was varied between 5 to 15 Å in steps of 5 Å. An Ar working pressure of 1.5 mTorr was used during deposition of all the stack layers, in an ultra-high vacuum chamber with base pressure below 5×10^{-9} Torr. Samples were annealed for a short time (60 s) in order to minimize diffusion, as in our previous report,[15] at temperatures ranging from 250 °C to 350 °C in step of 50 °C. During the annealing process, N_2 gas with 1 sccm flow rate was used to avoid the oxidation. The properties of the thin films (un-patterned) PSV films were studied using alternating gradient magnetometer (AGM), XRD, a dc-four-point probe with magnetic field applied perpendicular to the film plane for current-in-plane (CIP) GMR measurements.

II. Results and Discussion

Figure 1 (a-d) show the magnetic hysteresis (MH) loops of PSV for different annealing temperatures with $Co_{20}Fe_{60}B_{20}$-SPL (M_s ~ 1300 emu/cc) and $Co_{60}Fe_{20}B_{20}$-SPL (M_s ~ 880 emu/cc). The thickness of SPL was fixed at 5 Å (a and c) and 10 Å (b and d). The M_s for $Co_{40}Fe_{40}B_{20}$ (~ 1150 emu/cc) is closer to the M_s

for $Co_{20}Fe_{60}B_{20}$. Thus, similar magnetic behavior, not shown in this paper, for the PSV films with the $Co_{40}Fe_{40}B_{20}$-SPL was observed.

Figure 1 (a, c, d) reveal sharp switching characteristics at the SL and HL and also large coercivity indicating that post annealing improves the PMA of the Co/Pd multilayers which is in agreement with our previous work.[15] However, weaker PMA is observed for the $Co_{20}Fe_{60}B_{20}$-SPL when the thickness is increased to 10 Å, as the soft layer magnetization was found to be canted from out-of-plane orientation. It is most likely could be explained to be due to the fact that M_s increases in Fe rich compositions of $Co_xFe_{80-x}B_{20}$ SPL (here M_s for $Co_{20}Fe_{60}B_{20}$-SPL is about 1300 emu/cc). This larger value in M_s leads to the larger shape anisotropy ($-NM_s$).

It is also interesting to note that with thicker $Co_{20}Fe_{60}B_{20}$-SPL, the hard magnetic layer shows two steps reversal; a faster switching after nucleation and a slower one near/after the coercive point. Similar behavior has been previously reported in granular CoCrPt:SiO_2 media with a significantly large exchange coupling due to poor segregation.[16] The sharp switching around nucleation field is due to the reversal of magnetization in certain regions, which reduces magnetostatic energy. The slower reversal near/after the coercive point is due to the energy required to overcome the demagnetization energy of a large number of domains,[17] resulting in increased tail at the saturation field.

Although there is a clear separation between the switching fields of the soft magnetic layer and hard magnetic layer for thinner SPLs, the samples with thicker CoFeB-SPL (15Å) did not show clear separation. This could be due to the exchange coupling between two layers with in-plane (CoFeB-SPL) and perpendicular anisotropy (Co/Pd bilayers).[18] Therefore, magnetization becomes increasingly tilted in such a way that the switching of the magnetizations of both the free and hard layers cannot be distinguished. As a result, no magnetoresistance could be obtained for this thickness at all the annealing temperatures.

Figure 2(a-d) shows the representative CIP-GMR curves of the PSV films for 5 Å and 10 Å of $Co_xFe_{80-x}B_{20}$-SPL. It can be noted that the as-deposited sample shows rectangular loops for x=20 at 5 Å. The GMR shows a slight increase after annealing at 250 °C. However, further annealing reduces the GMR. Moreover, annealing at all temperatures lead to a tail towards saturation. For x=20, at 1 nm, the observed GMR is very low for the as-deposited sample. However, GMR shows a large increase after annealing at 250 degrees. It can be seen that further annealing reduces the GMR. Moreover, the GMR loop is not neatly rectangular and not showing sharp switching at the soft and hard magnetic layers. A shoulder from the soft layer reversal and a tail from the hard layer reversal are observed when the field is increased from zero and towards the saturation. A similar observation is observed for x = 40 and x = 60 samples, as well. However, x = 60 samples did not show a remarkable shoulder in the soft layer reversal. Except for the samples with x = 20, all the samples showed a dramatic increase in GMR after annealing at 250 degrees. These results are, however, in contrast with what is usually expected in PSV structures as it is generally believed that the GMR would decrease after annealing at high temperatures.

It was supposed that GMR degradation with increase of SPL thickness could be due to the poor quality of certain SPL in the as-deposited state. The validity of this speculation is further strengthened by the observation that the increase in GMR after annealing is more dramatic for thicker layers of SPL. As annealing is believed to improve the film/interface quality, it is thought that the quality of SPL at the interface improves with annealing. Therefore, the resistivity of the $Co_xFe_{80-x}B_{20}$-SPL was measured in order to confirm this presumption. In the as-deposited state, the SPL with x = 20 exhibited large resistivity of about 435.7 μΩ.cm while the resistivity dropped to about 175 μΩ.cm, after annealing. For SPL with x = 60, the resistivity was found to decay from 215 μΩ.cm, for as- deposited sample, to 125 μΩ.cm for the annealed sample. Comparing these two samples, it can be noticed that the sample with the highest resistance in the as deposited state showed the lowest GMR. The GMR in the annealed states also correlate with the resistivity after annealing. Therefore, the difference between SPL resistivity could be one reason for achieving different MR signals. Accordingly, these results verify that the lower GMR ratio for the as-deposited films is mainly due to the poorer quality of the CoFeB films-especially for those with Fe rich compositions.

It is worthwhile to note that there is a faster degradation of GMR, for the films post annealed beyond 250 °C, as shown in Figure 2. This could have two possible reasons: firstly, this could be due to possible changes in the crystallographic properties after annealing; secondly, this could be due to possible reduction in spin polarization because of the interlayer diffusion upon annealing. Therefore, for insight into understanding the mechanism responsible for the degradation of magnetic and transport properties of PSV with higher annealing temperature, two more measurements were conducted. The first step towards understanding the effect of annealing on magnetic behavior of the samples is done by quantification of ferromagnetic interlayer coupling strength via the minor loop shift of the soft layer switching for different annealing conductions. The minor loop shift would be simply obtained from MH loops, as shown in Figure 3(a). Figure 3(b), reveals an increase in the interlayer coupling field only for the samples annealed above 300 ºC. This increase in interlayer coupling can be attributed to the diffusion of $Co_xFe_{80-x}B_{20}$ and Cu at the spacer layer interfaces[12] and also indicates that the rate of diffusion at the Cu spacer layer interfaces is similar to the rate of intermixing between the $Co_xFe_{80-x}B_{20}$ and Pd layers for a 20 Å thick Cu spacer layer. Exchange coupling has a dramatic increase for PSV samples with 10 Å of $Co_{60}Fe_{20}B_{20}$ spin polarizer. This is further evidence for the maximum diffusion between SPL with Co rich composition and Cu spacer layer.

In order to confirm if the GMR decay, upon post annealing beyond 250 ºC, is dominated by the spin polarization reduction due to Pd diffusion within the entire Co/Pd multilayer stack, or into the $Co_{80-x}Fe_x$ spin filters, the temperature dependence of the hard and soft magnetic layers coercivities and sheet resistances for different annealing temperatures was investigated. Figure 4 shows the coercivity of soft and hard magnetic layers as a function of annealing temperatures for different thicknesses of $Co_xFe_{80-x}B_{20}$. This figure also shows that post annealing further increases the PMA of the magnetic layers. Clearly, it could be concluded that both SL and HL coercivity values increase with increasing the annealing temperature. Moreover, the increase of sheet resistance by 7.3%, 19.5% and 31.7% at annealing temperatures of 250 °C, 300 °C and 350 °C, respectively, provide further evidence that inter-diffusion within the layers (e.g. bilayers of Co and Pd as well as $Co_{80-x}Fe_x$ and Cu) is one of the main causes of GMR degradation. Once again it could be highlighted that GMR decreases after post annealing beyond 250 ºC while sheet resistance increases. However, there is a peak in GMR for the samples annealed at 250 ºC compared to as-deposited samples.

It is known that, fcc (111) orientation of Co/Pd multilayers is crucial to obtain PMA. Therefore, rocking curve measurements were conducted at CoPd (111) angle, in order to study whether or not there is any correlation between GMR and texture quality. Figure 5 shows the dependence of GMR on the FWHM of the rocking curve ($\Delta\theta_{50}$) of the CoPd (111) peak for different $Co_{60}Fe_{20}B_{20}$ thicknesses. The results indicate that samples with stronger and narrower Pd (111) peak intensity with a smaller $\Delta\theta_{50}$ at the mentioned peak position produces larger GMR signals. Strongest PMA were observed for the samples annealed at 250 ºC, where it has also the largest value for the GMR signal. This could be resulting from the improved PMA after annealing. This PMA is stronger for the thicker SPL, compared to thinner ones, because the hard layer is deposited above the two bilayers of Co/Pd including 10Å of CoFeB SPL and the Cu spacer layer, allowing sufficient development of the fcc (111) for the hard layer such that the alloy formed from interdiffusion does not destroy the PMA. Although interesting, it is quite possible that this effect may not be seen at device levels, when the magnetic layers are at the single-domain state after patterning. However, such a texture effect may result in a device-to-device variation in the switching current and GMR values when the device size is scaled down. It is necessary to achieve uniform texture over the whole surface to minimize such a distribution.

To conclude, CoFeB with 60:20:20 atomic composition is proposed to be used in PSV structures as it shows the lowest M_s leading to the lower demagnetization filed and therefore stronger PMA. It also shows larger GMR signal and low switching field for the soft layer, both promising for being used in device structures. However, to propose the most appropriate CoFeB composition for being used in p-MTJ devices, Cu spacer layer is necessary to be replaced with MgO tunnel barrier which would be our future interest of study.

ACKNOWLEDGMENT

T. Tahmasebi expresses gratitude for the support from the A*STAR (SINGA) program.

References

[1] R. D. Gomez, T. V. Luu, A. O. Pak, K. J. Kirk, and J. N. Chapman, J. Appl. Phys. **85**, 6163 (1999).

[2] R. Sbiaa, H. Meng and S.N. Piramanayagam, Phys. Status Solidi RRL **5**, 413 (2011).

[3] An-Cheng Sun, P. C. Kuo, Jen-Hwa Hsu, H. L. Huang, and Jui-Ming Sun, J. Appl. Phys. **98**, 076109 (2005).

[4] T. Tahmasebi, S.N. Piramanayagam, R. Sbiaa, H.K. Tan, R. Law, S. Lua, T. C. Chong, Phys. Status Solidi RRL **5**, 426 (2011).

[5] H. Kurt, R. Loloee, K. Eid, J. Pratt, and J. Bass, Appl. Phys. Lett. **81**, 4787 (2002).

[6] S. Yuasa, A. Fukushima, H. Kubota, Y. Suzuki, and K. Ando, Appl. Phys. Lett. **89**, 042505 (2006).

[7] A. Kharmouche, S. M. Cherif, A. Bourzami, A. Layadi, and G. Schmerber, J. Phys. D., **37**, 2583 (2004).

[8] R. Law, R. Sbiaa, T. Liew, and T. C. Chong, Appl. Phys. Lett., **91**, 242504 (2007).

[9] M. Li, G. C. Wang, and H. G. Min, J. Appl. Phys., **83**, 5313 (1998).

[10] A. Sharma, R. Brajpuriya, S. Tripathi, D. Jain, R. Dubey, T. Shripathi, and S. M. Chaudhari, Mater. Sci. Eng. B, **130**, 120 (2006).

[11] T. Tahmasebi, S.N. Piramanayagam, R. Sbiaa, R. Law, T. C. Chong, IEEE Trans. Magn., **46**, 1933 (2010).

[12] R. Law, R. Sbiaa, T. Liew and T. C. Chong, IEEE Trans. Magn., **44**, 2612 (2008).

[13] J. H. Chang, H. H. Chen, and C. R. Chang, Phys. Rev. B **83**, 054425 (2011).

[14] S. X. Huang, T. Y. Chen, and C. L. Chien, Appl. Phys. Lett. **92**, 242509 (2008).

[15] T. Tahmasebi, S. N. Piramanayagam, R. Sbiaa, R. Law, T. C. Chong, J. Nanosci. Nanotechnol. **13**, 2661 (2010).

[16] K. Srinivasan, S.N. Piramanayagam, R. Sbiaa and R.W. Chantrell al., J. Magn. Magn. Mater. **320**, 3041 (2008).

[17] R. Sbiaa, Z. Billin, M. Ranjbar, H. K. Tan, S. J. Wong, S. N. Piramanayagam and T. C. Chong, J. Appl. Phys. **107**, 103901 (2010).

[18] R. Sbiaa, H. Le Gall, Y. Braik, J.M. Desvignes and S. Yurchenko, IEEE Trans. Magn., **31**, 3274 (1995).

Figure Captions

Fig. 1. (Color online) Magnetic hysteresis curves of as-deposited and annealed Co/Pd-based PSVs. a) 5Å of $Co_{20}Fe_{60}B_{20}$, b) 10Å of $Co_{20}Fe_{60}B_{20}$, c) 5Å of $Co_{60}Fe_{20}B_{20}$, d) 10Å of $Co_{60}Fe_{20}B_{20}$.

Fig. 2. (Color online) GMR curves of as-deposited and annealed PSVs based on $[Co(6Å)/Pd(8Å)]_2$ multilayer with a pin polarizer layer of (a) 5Å of $Co_{20}Fe_{60}B_{20}$ and (b) 10Å of $Co_{20}Fe_{60}B_{20}$, (c) 5Å of $Co_{60}Fe_{20}B_{20}$ and (d) 10Å of $Co_{60}Fe_{20}B_{20}$.

Fig. 3 (a). (Color online) Minor loop shift of the soft layer switching in magnetic hysteresis loops.

Fig. 3 (b). (Color online) Interlayer coupling field between the magnetic layers versus annealing temperatures.

Fig. 4. (Color online) Magnetic layers coercivity versus annealing temperature for different M_s and different thicknesses of $Co_xFe_{80-x}B_{20}$ spin polarizer layer.

Fig. 5. (Color online) GMR dependence with FWHM for as-deposited and annealed Co/Pd-based PSVs with 5Å and 10Å of $Co_{60}Fe_{20}B_{20}$ polarizer.

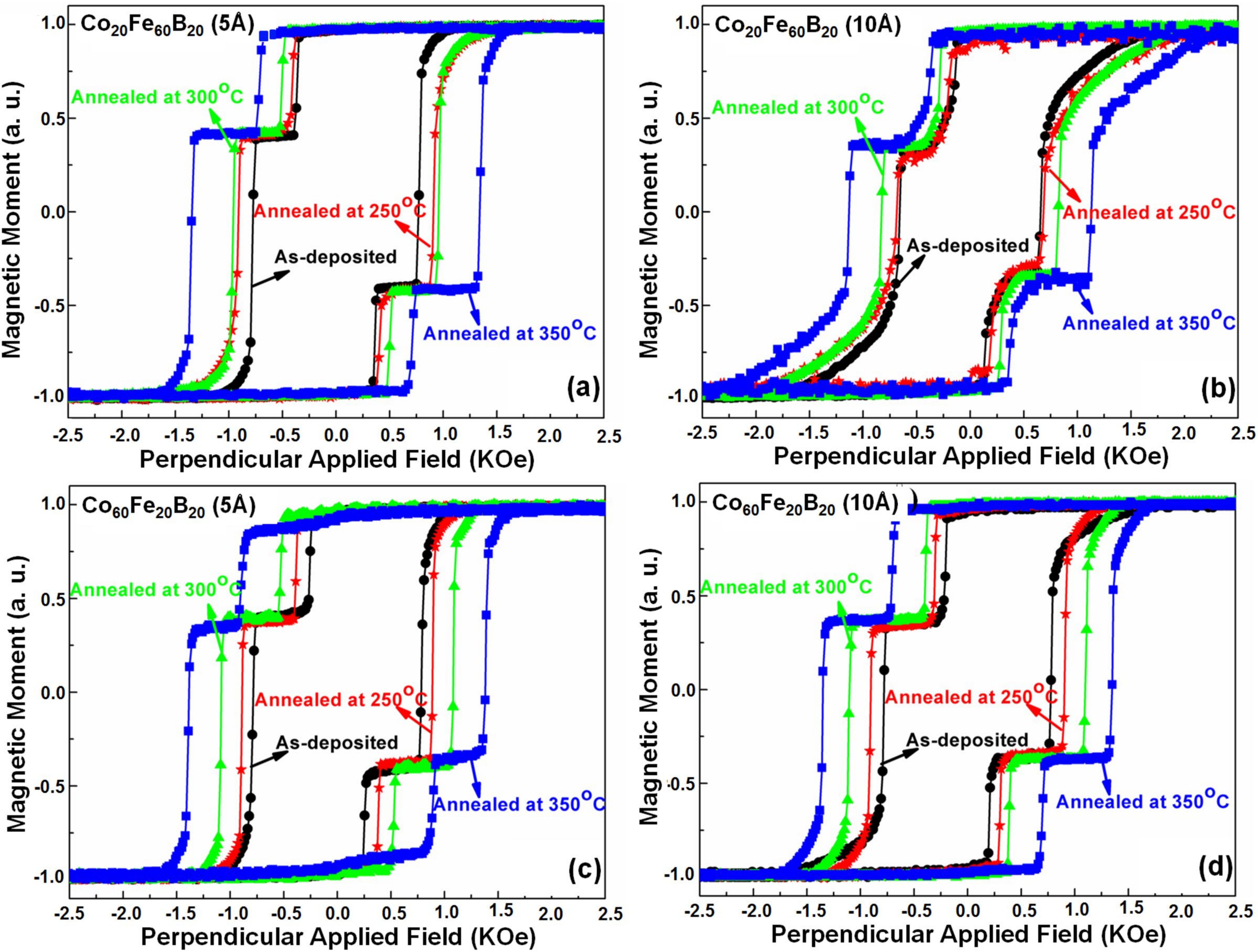

Co20Fe60B20 (5Å)
Annealed at 300OC
Annealed at 250OC
As-deposited
Annealed at 350OC
(a)
Co20Fe60B20 (10Å)
Annealed at 300OC
Annealed at 250OC
As-deposited
Annealed at 350OC
(b)
Co60Fe20B20 (5Å)
Annealed at 300OC
Annealed at 250OC
As-deposited
Annealed at 350OC
(c)
Co60Fe20B20 (10Å)
Annealed at 300OC
Annealed at 250OC
As-deposited
Annealed at 350OC
(d)
Magnetic Moment (a. u.)
Perpendicular Applied Field (KOe)

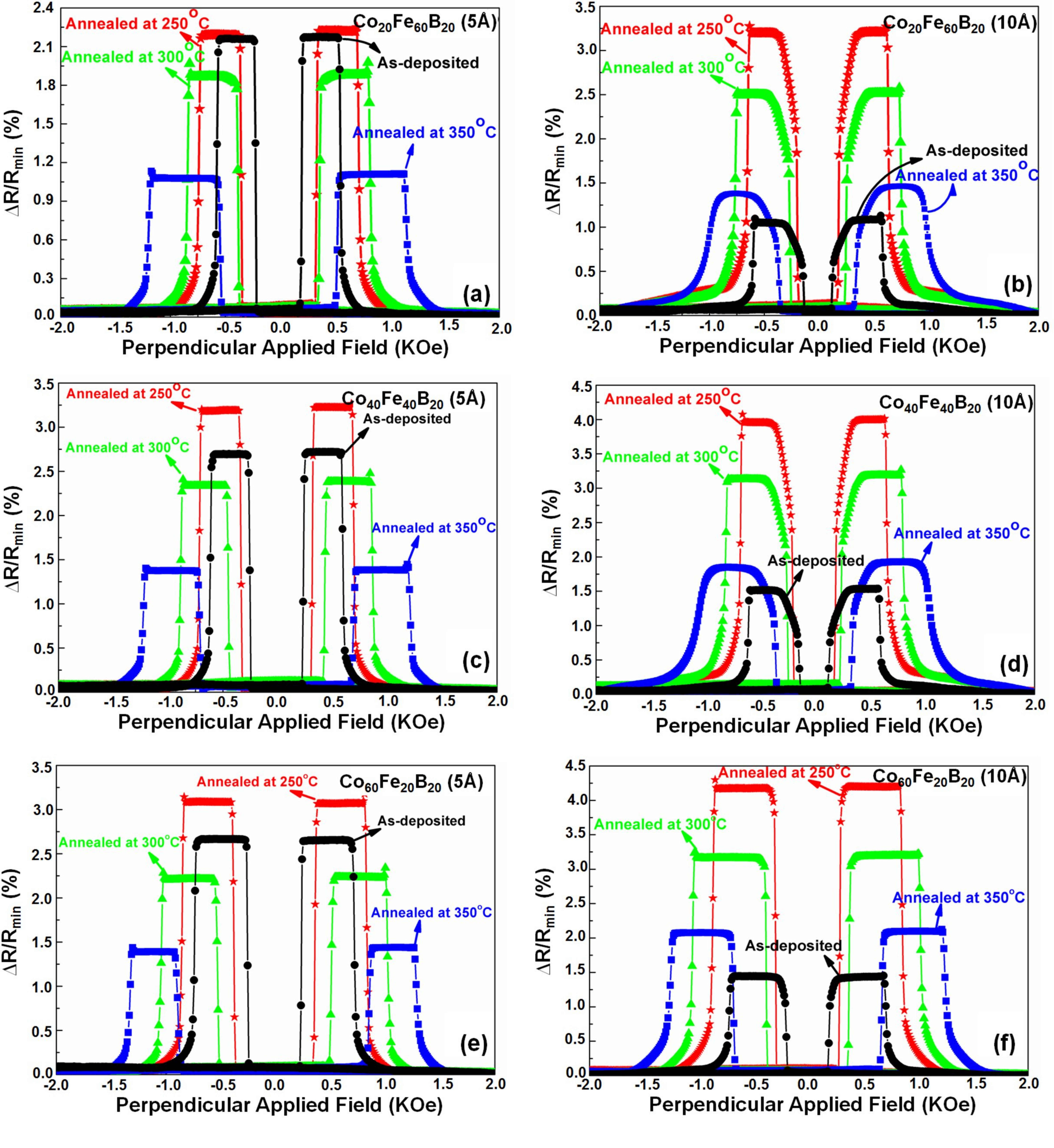

Co20Fe60B20 (5Å)
Annealed at 250°C
Annealed at 300°C
Annealed at 350°C
As-deposited
(a)
Co20Fe60B20 (10Å)
Annealed at 250°C
Annealed at 300°C
Annealed at 350°C
As-deposited
(b)
Co40Fe40B20 (5Å)
Annealed at 250°C
Annealed at 300°C
Annealed at 350°C
As-deposited
(c)
Co40Fe40B20 (10Å)
Annealed at 250°C
Annealed at 300°C
Annealed at 350°C
As-deposited
(d)
Co60Fe20B20 (5Å)
Annealed at 250°C
Annealed at 300°C
Annealed at 350°C
As-deposited
(e)
Co60Fe20B20 (10Å)
Annealed at 250°C
Annealed at 300°C
Annealed at 350°C
As-deposited
(f)
ΔR/Rmin (%)
Perpendicular Applied Field (KOe)

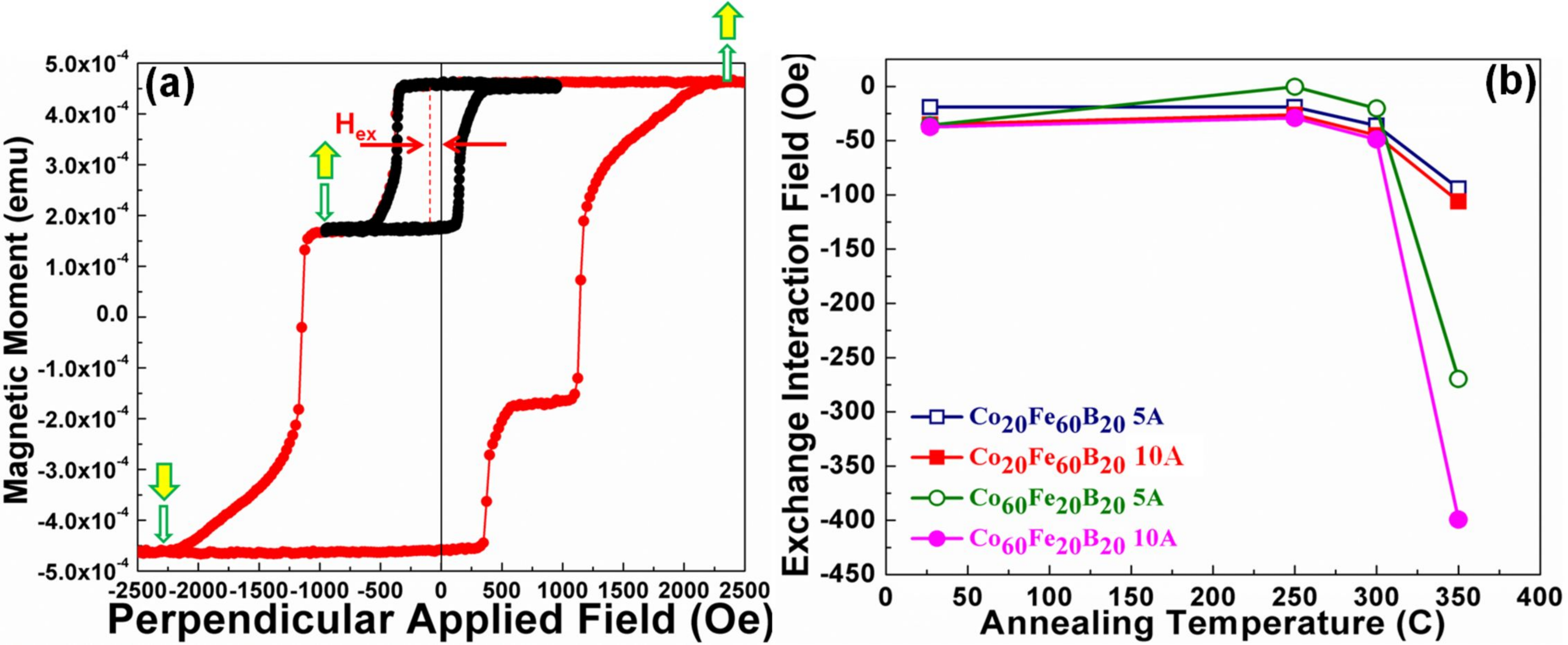
(a)
Magnetic Moment (emu)
5.0x10^-4
4.0x10^-4
3.0x10^-4
2.0x10^-4
1.0x10^-4
0.0
-1.0x10^-4
-2.0x10^-4
-3.0x10^-4
-4.0x10^-4
-5.0x10^-4
H_ex
-2500 -2000 -1500 -1000 -500 0 500 1000 1500 2000 2500
Perpendicular Applied Field (Oe)
(b)
Exchange Interaction Field (Oe)
0
-50
-100
-150
-200
-250
-300
-350
-400
-450
Co20Fe60B20 5A
Co20Fe60B20 10A
Co60Fe20B20 5A
Co60Fe20B20 10A
0 50 100 150 200 250 300 350 400
Annealing Temperature (C)

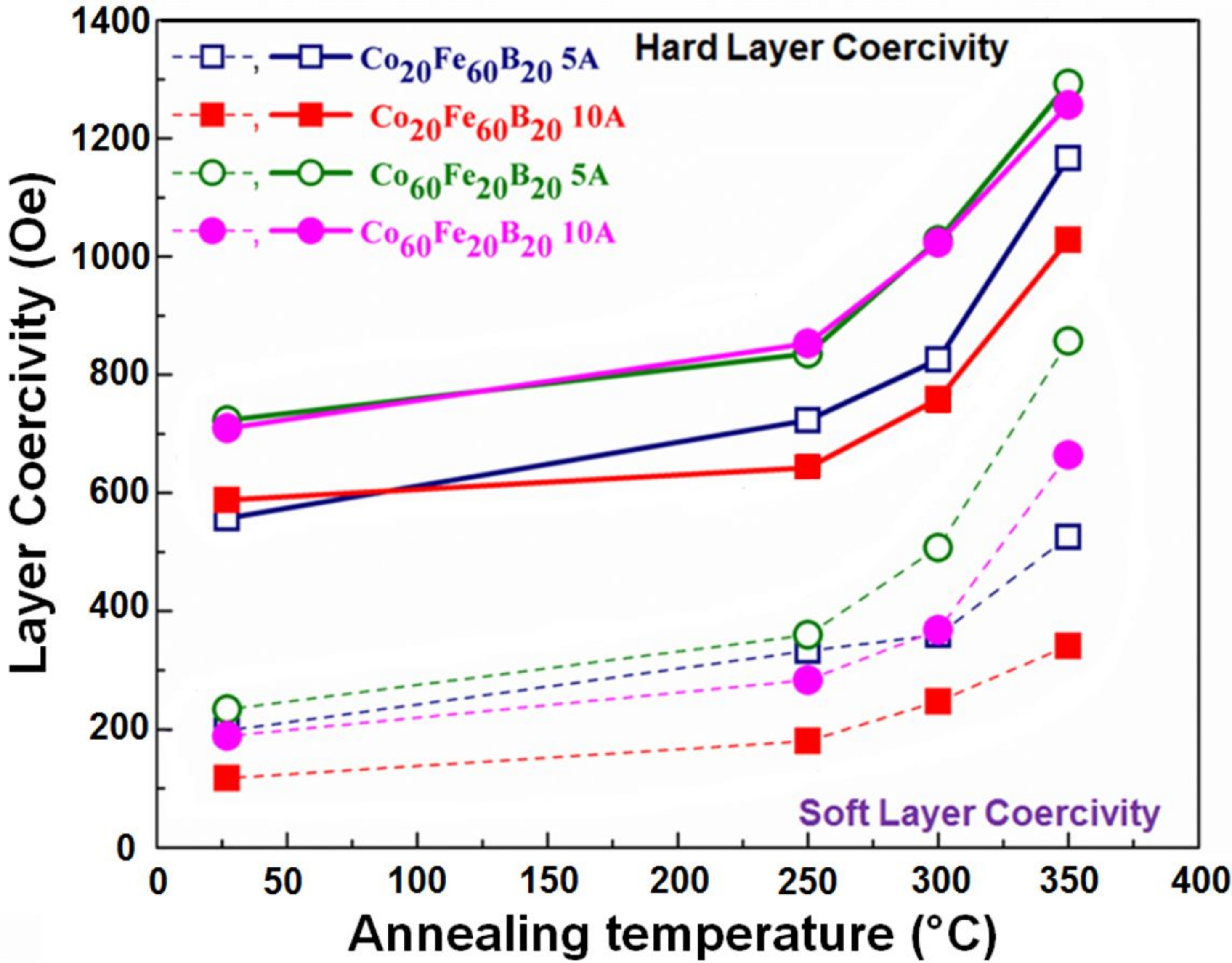

Hard Layer Coercivity
Soft Layer Coercivity
$Co_{20}Fe_{60}B_{20}$ 5A
$Co_{20}Fe_{60}B_{20}$ 10A
$Co_{60}Fe_{20}B_{20}$ 5A
$Co_{60}Fe_{20}B_{20}$ 10A
Layer Coercivity (Oe)
Annealing temperature (°C)
0
200
400
600
800
1000
1200
1400
0
50
100
150
200
250
300
350
400

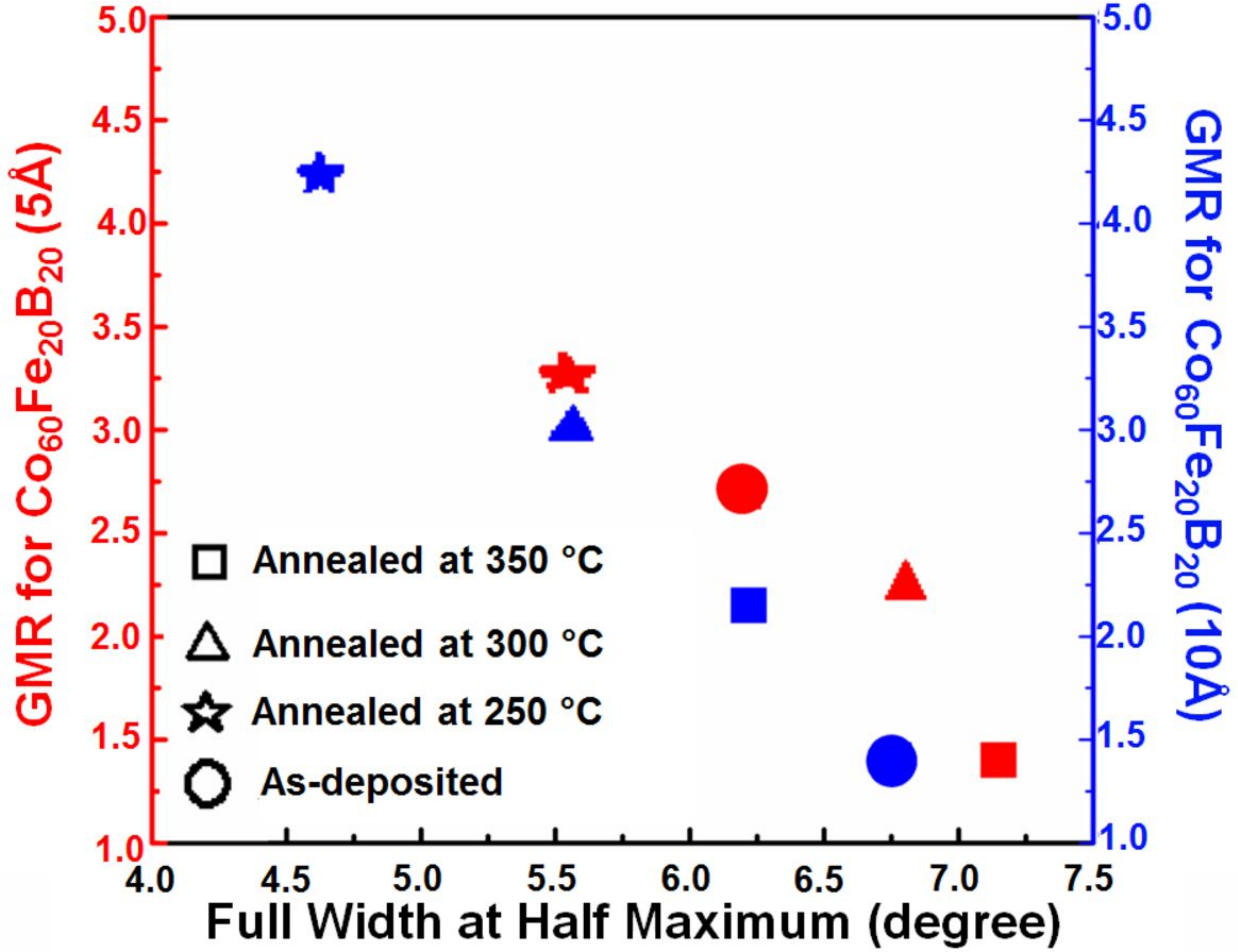

GMR for $Co_{60}Fe_{20}B_{20}$ (5Å)
GMR for $Co_{60}Fe_{20}B_{20}$ (10Å)
Full Width at Half Maximum (degree)
Annealed at 350 °C
Annealed at 300 °C
Annealed at 250 °C
As-deposited
1.0
1.5
2.0
2.5
3.0
3.5
4.0
4.5
5.0
4.0
4.5
5.0
5.5
6.0
6.5
7.0
7.5